RSC Advances

Studies on varying n-alkanethiol chain lengths on gold coated surface and their effect on antibody-antigen binding efficiency

SCHOLARONE™
Manuscripts

ROYAL SOCIETY
OF CHEMISTRY

Journal Name

ARTICLE

Studies on varying *n*-alkanethiol chain lengths on gold coated surface and their effect on antibody-antigen binding efficiency

P.Bhadra[a], M.S.Shajahan[a], E.Bhattacharya[a,b], A. Chadha [a,c,d*]

Self-assembled monolayer (SAM) of n-alkanethiols of different chain lengths (n=2, 3, 6, 11, 16) on gold surface are used to immobilize antibodies which in turn bind to antigen. The antibody and antigen used in this study have similar molecular weight i.e. ~150 kDa. The antibody [1.5µg/cm2] immobilized varied with the surface packing density of SAM of carboxylic acid-terminated n-alkanethiols of different lengths. On comparison, the efficiency of antibody immobilization was lowest on loosely packed SAM of n-alkanethiols (n≤3) and the highest on densely packed SAM of n-alkanethiols (n≥11). However, increased immobilization of antibody with increasing chain length of the n-alkanethiols [n>11], did not result in a corresponding increase in antigen binding. An attempt to explain this phenomenon based on packing density and an orientation of the captured antibody is presented.

1 Introduction

The generation of a specific antibody to an antigen and their interaction forms the basis of disease diagnostics and biosensor applications. In order to fabricate a highly reproducible and efficient biosensor, it is important to maximize interactions between antibodies and antigens. One method to do this is to control the density of the ligands [antibodies] on the surface of the biosensor, which are bound to linker molecules (*n*-alkanethiols) and which also bind to the specific antigen [1]. The reaction efficiency depends on the density of available reactive groups of the ligand [antibody] which are bound to the surface through the linker molecules [2]. Antibodies (which are used to bind antigens) are immobilized with specific orientations on to different supports for the purpose of better antigen binding [1-3]. However, when the antibody is first immobilized, the antigen binding efficiency to the antibody is very often reduced [4]. This is because the antigen binding to the immobilized antibody depends on the orientation of the antibody [5, 6]. A solution to this problem is the use of antigen binding fragments alone which can be isolated from whole antibody. This yields higher surface densities with more specific orientation of the antibody fragment, owing to the exposed nucleophilic sulfide, compared

to that of whole antibody itself. However, the immobilization process for these fragments is more challenging than employing whole antibodies [3]. As is well known, an antibody can adopt four different molecular orientations on the solid surface: "End-On"- fragment crystallizable region (Fc) attached to the support, "Head-On"- fragment antigen-binding regions (Fab) attached to the support, "Side-On"- one Fc and one Fab attached to the support, and "Flat-On"- all three fragments attached to the support [7]. In many cases, the actual antibody orientation on a given surface may be a combination of these. Clearly, the "End-on" orientation gives the most efficient antigen binding if the Fab is oriented towards the analyte side[8-11].

Even though SAM of different head groups and chain lengths are reported for different applications [9, 12-18] the question of optimal quantitative binding of SAM and antibody –antigen interaction is not addressed as in this study. Among them, *n*-alkanethiol SAM is of interest for biosensor applications. Hetero-functional *n*-alkanethiol (HS(CH$_2$)$_n$COOH, *n*≥1)SAM, consisting of a carboxylic acid at one end and thiol at the other end, are known to form a well packed monolayer on gold surface [19-21]. Porter *et.al* have reported in detail the packing density arrangement of thiols, especially, the disorder of SAM films for short chains (*n*<8) and crystalline like order in SAM films of longer chains (*n*>10) [21, 22]. It is to be expected that the higher packing density of SAM causes steric hindrance and in turn affects the binding efficiency of the incoming protein [8, 9]. In fact, loose packing of adsorbed antibody shows better antigen binding efficiency while the subsequent increase of surface-adsorbed antibody causes crowding or overlapping of antibody fragments thereby reducing antigen binding due to steric hindrance (Zhao *et al*[8] and Xu *et al*[9]). Also, densely packed antibodies on the surface are prone to steric problems

[a.] *Centre for NEMS and Nanophotonics, Indian Institute of Technology Madras, Chennai 600 036, India*
[b.] *Department of Electrical Engineering, Indian Institute of Technology Madras, Chennai 600 036, India*
[c.] *Department of Biotechnology,Indian Institute of Technology Madras, Chennai 600 036, India. E.mail: anjuc@iitm.ac.in; Tel: +91-44-2257-4106*
[d.] *National Centre for Catalysis Research, Indian Institute of Technology Madras, Chennai 600 036, India*

such that the immobilized antibody too is not permitted to protrude far enough into the solution for capturing the antigen [8, 9, 23]. However, till date, there is no systematic study on antibody immobilization efficiency with respect to different chain lengths of *n*-alkanethiols and subsequent antigen binding. This paper reports the effect of SAM of different lengths of *n*-alkanethiol linkers, binding of antibodies on the linker activated solid sample and the binding of antigen to the immobilized antibodies, thus correlating the lengths of *n*-alkanethiols and antigen binding *via* antibodies.

2 Materials and methods

2.1 Materials

Thioglycolic acid (TGA) (≥ 98%), 3-Mercaptopropionic acid (3MPA) (99%), 6-Mercaptohexanoic acid (6MHA) (90%),11-Mercaptoundecanoic acid (11MUA) (98%), 16-Mercaptohexadecanoic acid (16MHDA) (90%), N-hydroxysuccinimide(98%), N-(3-dimethylaminopropyl)-N'-ethylcarbodiimide, Ethanolamine(redistilled, ≥ 99.5%), Human immunoglobulin γ (HIgG) (reagent grade, ≥ 95% SDS PAGE, from human serum), Mouse monoclonal anti-human IgG(MIgG) (from mouse ascites fluid) , Anti-Mouse IgG-Peroxidase tagged antibody (Peroxidase-GIgG) (developed in goat), Anti-Mouse IgG-FITC tagged antibody (FITC-GIgG) (developed in goat). All chemicals and materials were purchased from Sigma-Aldrich unless stated. The 3, 3', 5, 5'-Tetramethylbenzidine substrate (TMB) assay kit was purchased from Thermo Scientific Pierce, USA.

2.2 Preparation of antibody-immobilized gold coated silicon sample

A p-type silicon wafer (100) was used as substrate. 5 nm chromium layer and 20 nm gold layer were sequentially deposited on the substrate through E-beam evaporation system (model no: BC-300T). This wafer was then diced into 1 cm x 1 cm size samples by ADT dicing instrument. Then individual samples were cleaned with acetone, isopropyl alcohol and finally rinsed with ethanol and deionized water. Now, individual samples were submerged in different ethanol solutions containing 1 mM of different chain length alkanethiol for 12hr. After the exposure period, the samples were washed in ethanol and deionized water. To covalently immobilize the antibody to the SAM adsorbed on the gold surface, the SAM was activated with a 1:1 volume mixture solution of 0.1 M N-hydroxysuccinimide (NHS) and HCl stabilized 0.4 M 1-ethyl-3-(3-dimethylaminopropyl)carbodiimide (EDC) for 1 hr at room temperature and finally washed with deionized water.

Theoretically, the amount of antibody molecules occupying $1cm^2$ surface is 4.06×10^{12} calculated by assuming that the dimension of the molecule from top view is 7.0nm × 3.5nm and forms a monolayer [24]. Converting this value in terms of mass, the approximate amount of antibody (molecular weight 150kDa) required is $1.2\mu g/cm^2$.Thus, 100 µl of the HIgG (15 µg/ml) in 10 mM phosphate buffered saline (PBS) solution (pH

7.4) was allowed to react with the surface activated samples for 12 hrs at 4 ^{0}C to covalently immobilize on it. Post reaction period, the samples were washed with PBS buffer containing 0.1% Tween 20 (PBST) followed by rinsing in PBS buffer. After antibody treatment, the samples were immersed in 1 M ethanolamine solution for 7 min to block all non-specific protein binding sites. Finally, the samples were washed with deionized water to remove unbound ethanolamine and were now ready for antigen binding.

2.3 Antigen binding on antibody terminated sample

A 100µl solution of MIgG (30µg/ml) in PBS buffer, acting as antigen, was pipetted on individual antibody coated sample and incubated for 3hr at 4^{0}C. 100µl of PBS buffer on antibody coated sample was used as a negative control. Finally, after incubation period the antigen terminated surfaces were washed thoroughly with PBST following with PBS.

2.4 Secondary antibody immobilization

For TMB substrate assay the prepared antigen-antibody immobilized samples were incubated with 100µl of Peroxidase-GIgG (30µg/ml) as secondary antibody in PBS buffer for 3hr at 4^{0}C in a dark ambience and washed thoroughly with PBST and PBS. For fluorescence spectroscopy the prepared antigen-antibody immobilized samples were incubated with 100µl of FITC-GIgG (30µg/ml) as secondary antibody in PBS buffer for 3hr at 4^{0}C in a dark ambience and washed thoroughly with PBST and PBS.

3 Experimental

3.1 SAM thickness estimation by spectroscopic ellipsometer

Spectroscopic ellipsometer (SE) is a characterization tool that can provide information regarding the immobilized layer thickness by measuring the changes in the reflectance and phase difference between the parallel and perpendicular components of a polarized light beam upon reflection from a surface [25, 26]. Substrates having flat and uniform surface (less roughness) reveal superior accuracy in thickness estimation [25]. The measured thicknesses generated using SE are generally expressed in terms of refractive index at a fixed wavelength of 632 nm.

3.2 Chemical immobilization of the antibody on a gold coated silicon substrate: Analysis by Attenuated Total Reflectance Fourier Transform Infrared Spectroscopy (ATR-FTIR)

To gain more detailed molecular bonding information regarding antibody immobilization on gold coated samples, ATR-FTIR measurement was performed [27]. The spectra were taken by averaging 20 scans at a resolution of 4 cm^{-1}. Reference spectrum was confined to the spectrum obtained with a bare silicon sample. All measurements were taken at room temperature.

ARTICLE

3.3 Estimation of antibody on SAM surface by Bicinchoninic assay (BCA)

The BCA protein assay is a detergent-compatible formulation based on bicinchoninic acid for the colorimetric detection and quantification of total protein which exhibits a strong absorbance at 562nm [28]. Here, a solution of HIgG was used as a standard to estimate the immobilized antibody.

3.4 Estimation of antigen by TMB substrate assay

TMB assay is a procedure employed by Theegala and Suleiman [29] for the quantification of antigen (MIgG) on solid sample. Samples with HIgG-MIgG and tagged secondary antibody [Peroxidase-GIgG] were placed in 5ml beakers. 250µl of TMB was pipetted and immediately placed on an orbital shaker (120rpm). Thereafter, 250µl of H_2O_2 and 0.1% of BSA in 500µl of PBS (pH7.4) were added. Basically, in presence of H_2O_2, the peroxidase enzyme oxidizes the colorless TMB to a blue colored product. The reaction was stopped with 100µl of 2M H_2SO_4 after 30min incubation period. Post 10min the absorbance of the solution was measured at 450nm. The amount of MIgG bound to HIgG was deduced from a standard assay with known concentration of MIgG.

3.5 Analysis of surface thickness measurements after antibody binding

The SE data in this case indicates the orientation of the immobilized antibody thereby providing information on antigen binding efficiency.

3.6 Atomic Force Microscopy (AFM) imaging of antibody on gold coated surfaces: Evidence of different alkanethiol chain length packing density and antibody orientation

Surface topology images of SAM of different chain length alkanethiols and immobilized antibody on the SAM layer were investigated with an AFM (BRUKER dimension edge) in contact mode. The scanning rate was modulated for 1Hz for upto 2.3 µm × 2.3 µm scale image. The image analysis was conducted with Gwyddion software where each micrograph was analyzed for average height and average surface roughness. The root mean square of the height variance (RMS) roughness value,

Rq, was generated through Gwyddion software using the inbuilt formula.

3.7 Antigen distribution on antibody terminated surface by fluorescence spectroscopy

Fluorescence spectra were obtained from HORIBA JOBIN YVON NanoLog Spectrofluorometer. FITC tagged secondary antibody (FITC-GIgG) that bound to the MIgG coated surface determines the distribution of antigen.

4 Results and discussion

4.1 SAM layer thickness by spectroscopic ellipsometer

Table 1 is the tabulated information on spectroscopic ellipsometer thicknesses measured for *n*-alkanethiol SAM. Here, the formation of single layer was confirmed with slight deviations from the expected value for all alkanethiol on gold coated samples. According to A. W. Snow *et al* and Frank Schreiber, this deviation is explained by the fact that SAM prepared from alkanethiol has an extended methylene chain conformation with a tilt angle from the surface normal and its terminal groups are situated at the air interface [2, 30].

4.2 Analysis by ATR-FTIR

The individual alkanethiols in ethanol show the –SH, –COOH and the routine bands due to –CH_2– groups at 2527 cm^{-1}; 1660 cm^{-1}, 1042 cm^{-1},1086 cm^{-1};and 1330 cm^{-1} as expected (Fig. 1) [1, 31]. The alkanethiols on Au (Fig. 2) show –COOH at 1696-1710 cm^{-1} (C=O), 1265 cm^{-1} and 1527 cm^{-1} (COO$^-$ stretching). The 2527 cm^{-1} weak band of –SH disappears after step I, indicating the formation of a new S–Au bond [32]. These bands prove that the *n*-alkanethiol molecules have bonded to the Au surface through the S–Au bond at one end while the carboxyl group is free at the other end to react with the NHS/EDC in step II[33]. The CH_2 asymmetric stretching band shifts towards a lower value i.e. from 2948 cm^{-1} to 2931cm^{-1}(Fig. 3) for increasing chain lengths of *n*-alkanethiols. This shift to lower values is due to increased van der Waals interaction between the methylene chains which indicates that 16MHDA SAM has a more well-ordered structure than TGA as a result of better surface packing density [31, 34].

Table 1 Surface layer thickness study of individual alkanethiol SAM on gold coated samples.

Sample	Chain length (*n*)	Thickness of monolayer (nm)	Measured thickness by Spectroscopic Ellipsometer (nm)
TGA	2	0.45 [35]	0.46 ± 0.03
3MPA	3	0.50 [36]	0.48 ± 0.02
6MHA	6	1.50 [31]	1.48 ± 0.04
11MUA	11	1.90 [37]	1.81 ± 0.03
16MHDA	16	2.50 [38]	2.39 ± 0.03
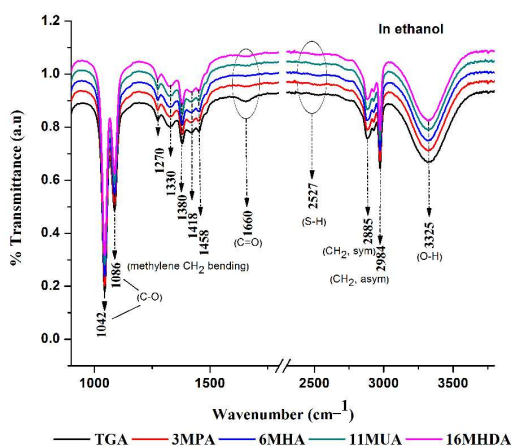
Fig. 1 FTIR spectra of individual alkanethiols in ethanol

Fig. 2 FTIR spectra of SAM of individual alkanethiols on Au surface

Fig. 3 CH$_2$ asymmetric stretching frequencies as determined by FTIR-ATR for different n-alkanethiols.
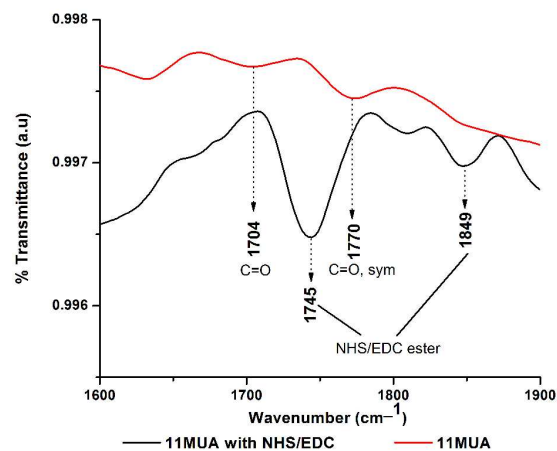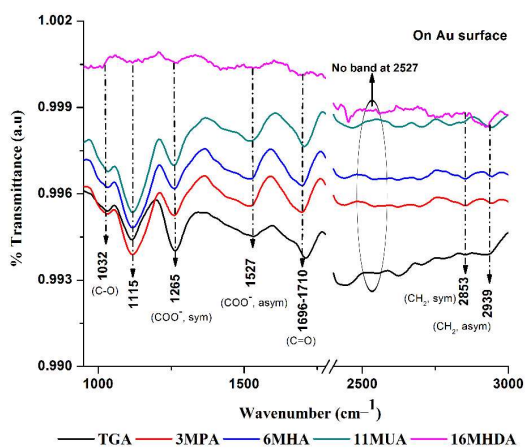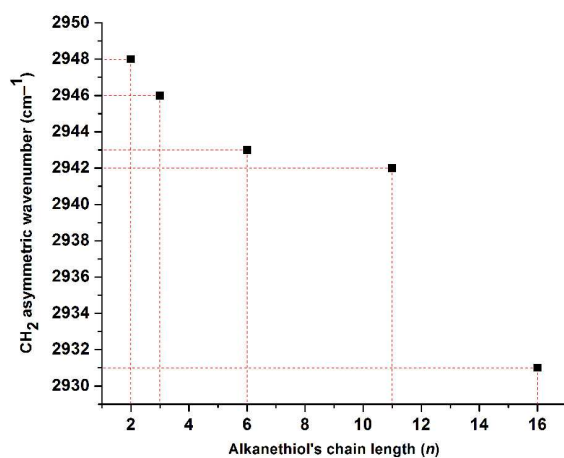

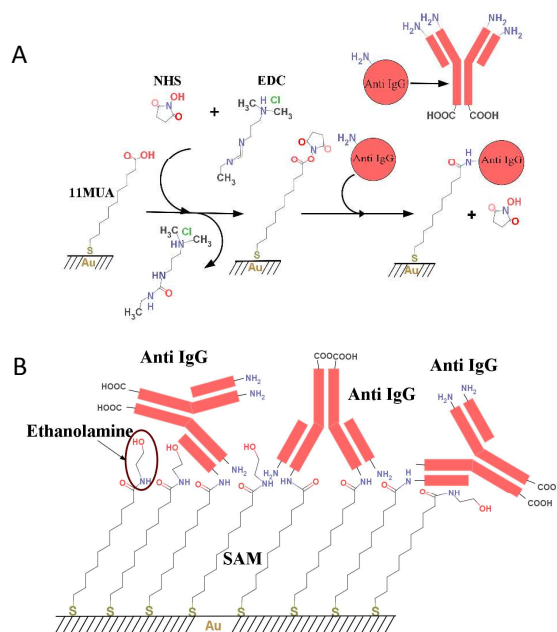Fig. 4 FTIR spectra comparison of 11MUA SAM before and after NHS/EDC activation

Fig. 5(A) An antibody is coupled to a gold coated silicon surface through EDC/NHS chemistry{adapted from [39]}.(B) Illustration of a gold coated silicon surface immobilized with antibody and blocked by ethanolamine. The diagrams were drawn with the software- Marvin Sketch.

The FTIR spectra of 11MUA before and after NHS/EDC activation is represented as an example for alkanethiol interaction prior to antibody molecule binding (Fig. 4). On NHS/EDC binding, the band at 1704 cm[-132], signature of C=O bond of the –COOH group of SAM on gold coated surface disappears indicating that 11MUA has reacted with NHS/EDC forming an ester intermediate as seen as strong bands centered at 1745 cm^{-1} and at 1849 cm[-140]. This intermediate NHS/EDC ester binds the antibody with SAM layer covalently (illustrated in Fig. 5).
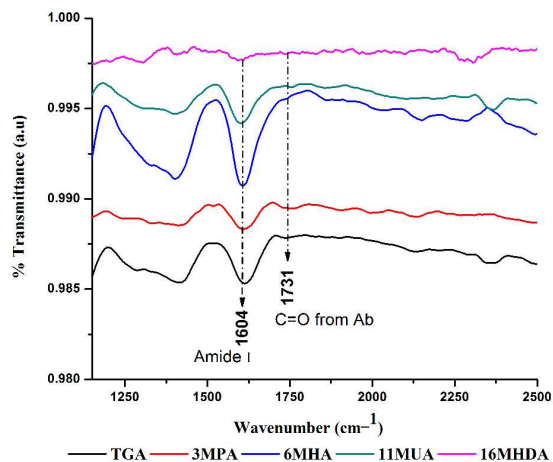
Fig. 6FTIR spectra of antibody covalently attached to different *n*-alkanethiol SAM, after surface activation with NHS/EDC.

Fig. 7 Antibody immobilized (estimated by BCA) and antigen-antibody binding (estimated by TMB assay) on different *n*-alkanethiol.

Fig. 6 shows the FTIR of antibody molecules immobilized *via* the NHS/EDC reactions for all alkanethiols. The absorption bands at 1500-1700cm^{-1} correspond to the expected specific amide bands i.e.Amide I at 1604 cm^{-1}. The bands at 1700-1750cm^{-1} are due to the –COOH groups of the antibody[40, 41]thus confirming antibody immobilization by covalent attachment and formation of the amide bond [42](Fig.6). The C=O band of –CONH at 1731 cm^{-1}was seen unchanged for all the chain lengths studied. The intensity of the amide bond increased with varying chain lengths of *n*-alkanethiols (from *n*=2-11). However, for *n*=16 chain length of *n*-alkanethiol SAM, the intensity of the band at 1731 cm^{-1}(COOH stretching) decreased. The reduction in the intensity of these bands indicate the structural changes of higher amount of antibody during covalent binding [40].

4.3 BCA and TMB assay analysis

Both the assays determine the concentration of proteins. The BCA assay is to estimate antibody immobilized on each sample and the antigen is estimated by the TMB assay. The antibody attached increases and reaches a saturation at *n*=11 chain length of *n*-alkanethiol SAM (Fig. 7).This trend is explained in terms of packing density of SAM evident from FTIR analysis .In the case of higher chain length SAM (*n*=6, 11, 16) the surface isclose-packed with fewer defects and better stabilized by van der Waals forces compared to that of lower chain length SAM (*n*=2, 3)[12, 16, 21, 22]. This leads to a more accommodating surface for antibody immobilization on these samples. The findings are illustrated in Fig.8. The estimation of antigen bound to the antibody terminated surface was performed by TMB substrate assay [43]. The amount of antigen captured by the antibody increases rapidly with the chain length *n*≥6 but no significant antigen binding differences were observed beyond *n*=11.(Fig. 7). It isreported that greater antigen binding activity is expected in the most densely packed and properly oriented antibody layer[44, 45].
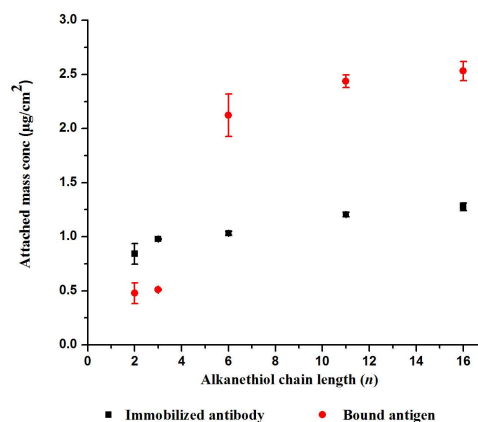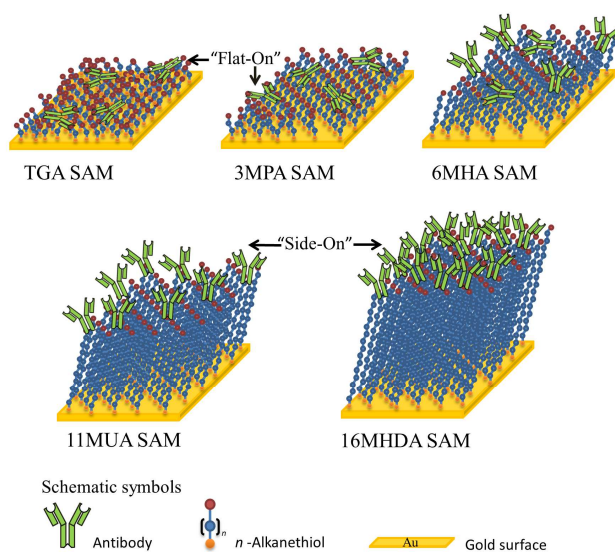

Fig. 8 Illustration of antibody attachment and orientation on the different *n*-alkanethiol SAM.

Thus packing density of *n*-alkanethiol influences the amount of antibody that is accommodated on the surface and its orientation, which in turn is reflected by the binding of antigen with the antibody. Thus, more antibodies need not necessarily mean more antigen.

4.4 Analysis of surface thickness measurement after antibody-antigen binding

The antibody-antigen interaction depends on the orientation of the antibody. A better antigen binding efficiency is obtained if the Fab are oriented in "End-On" manner, but the amide bond which is formed between the SAM –COOH and the –NH$_2$ group of the antibody is possible only in the 'Side-On' orientation.

Table 2 Spectroscopy thickness study of HIgG antibody on individual alkanethiol SAM

Sample (1cm^2 wafer)	Chain length (n)	Thickness measurement of antibody by SE (nm)
TGA	2	3.02 ± 1.26
3MPA	3	3.42 ± 1.62
6MHA	6	5.42 ± 1.65
11MUA	11	9.8 ± 2.8
16MHDA	16	9.76 ± 2.25

Spectroscopic ellipsometer (SE) is a useful tool for determining the orientation of the antibody [46]. IgG is approximated as an ellipsoid shape with 14nm long axis and 4nm short axis [47]. Here, the IgG orientation and structure is not controlled by an external force but rather by its own interaction with the SAM layer.

The SE analysis of antibody attached on different n-alkanethiol SAM for the purpose of investigating the orientation of the antibody is presented in Table 2. It was established that the different n-alkanethiols form SAM on gold coated surface (Table 1). In case of TGA and 3MPA coated surfaces the obtained thicknesses after antibody attachment is similar i.e. 3.02 ± 1.26nm and 3.42 ± 1.62nm, respectively. In case of 11MUA and 16MHDA, a 3-fold increase is seen in the thickness i.e. 9.8 ± 2.8 nm and 9.76 ± 2.25 nm as compared to that of TGA and 3MPA. This reflects that the antibody orientation strongly depends on the chain length of the underneath SAM layer. In case of both TGA and 3MPA SAM, antibody is presumed to bind to the surface in a "Flat-On" manner. From 6MHA SAM coated surface onwards the antibody thickness increases (Table 2) implying onset of "Side-On" antibody orientation due to packing density. SAM packing density is higher 6MHA onwards compared to that of TGA and 3MPA (subsection 4.2 and 4.3) thus orienting the antibody to bind in the preferred "Side-On" manner. It is not because of structural deformity that the thickness increases since TMB assay shows that the antigen binding efficiency of 6MHA, 11MUA and 16MHDA is higher compared to that of TGA SAM and 3MPA SAM coated surface (subsection 4.3). Structurally deformed and randomly oriented antibodies have poor binding activity [48].

4.5 Surface topography analysis by AFM

Height histogram data was extracted from AFM topographical images of antibody molecules on SAM surfaces using the Gwyddion software [49], presented in ESI†. Average height and average surface roughness (RMS) parameters were estimated and tabulated in order to compare the topography of each SAM of different chain length alkanethiol surfaces. Average height for each SAM (Table 3) correlates well with SE thickness data from Table 1 thereby confirming the formation of a monolayer. The estimated RMS for bare gold surface [control] was 1.2 nm and the RMS for the individual SAM on gold surface reduced from 1.4 nm to 0.3nm as the chain length increased from n=2 to n=16. RMS is generated due to the defects formed during the processing (immobilization stage)[50]. Highly ordered and dense packed SAM have fewer defects and are better stabilized by van der Waals forces. Thus higher chain length SAM (n≥6) showed low RMS value compared to the lower chain length SAM (n≤3).

Similarly, the orientation of the antibody on SAMs of different chain lengths of alkanethiol was also investigated by AFM analysis. Green *et al.*[51] and Schramm *et al*[52] have shown that since the length and width of antibody is different, different orientations result in the changes in surface topography in terms of average height and surface roughness. Comparing SAM before and after antibody immobilization provided further insight into orientation of the antibody. For example, in TGA the average height increased from 0.46 ± 0.03 nm to 2.5 ± 0.55 nm and the surface roughness from 1.4 nm to 2 nm after antibody immobilization. This indicated that the antibody molecules immobilized on TGA coated surface prefer a "Flat-On" orientation. On the other hand in case of 11MUA the average height increased from 1.81 ± 0.03 to 10.54 ± 1.92 and surface roughness from 0.5 nm and 3.5 nm after antibody immobilization. This indicated that antibody molecules immobilized on 11MUA coated surface prefer a "Side-On" orientation. These AFM results further corroborated the antibody orientation results (subsections 4.3 and 4.4).

Table 3: Data acquired by AFM and analysed by Gwyddion software

Sample	Average surface roughness (RMS) (nm)	Average height (nm)	Sample	Average surface roughness (RMS) (nm)	Average height (nm)	Orientation
TGA	1.4	0.46 ± 0.03	Ab-TGA	2	2.50 ± 0.55	"Flat-On"
3MPA	1.1	0.48 ± 0.02	Ab-3MPA	2.3	3.36 ± 0.7	"Flat-On"
6MHA	0.7	1.48 ± 0.04	Ab-6MHA	3.3	5.06 ± 1.66	"Side-On"
11MUA	0.5	1.81 ± 0.03	Ab-11MUA	3.5	10.54 ± 1.92	"Side-On"
16MHDA	0.3	2.39 ± 0.03	Ab-16MHDA	3.8	9.25 ± 0.66	"Side-On"

Ab – Antibody immobilized to respective SAM

4.5 Fluorescence spectroscopy analysis

Fluorescence spectroscopy is used to estimate the amount of antigen on the surface *via* the FITC-GIgG. Fig.9shows the fluorescence emission spectra of FITC-GIgG on different *n*-alkanethiols. In general fluorescence intensity is a function of concentration of the fluorophore as defined by the Beer–Lambert's law. Here, the excitation wavelength was at 480nm and the emission maxima was recorded at 527nm[53]. Fluorescence intensity increased with the variation in *n*-alkanethiol chain length and no change in the wavelength of the emission maxima was observed. In lower chain length TGA, the attached antibodies as well as antigen are less, suggesting a loosely packed surface. The surface packing density increases with higher chain length *n*-alkanethiols, confirming the results already obtained by BCA and TMB assay. However, the intensity dropped drastically in the case of 16MHDA. The possible reason for this change in fluorescence intensity is attributed to self-quenching [54]. As seen in subsection 4.3, 11MUA is the saturation point in antibody and antigen binding therefore 11MUA and 16MHDA should show similar peak intensity. However this is not the case, as 16MHDA has higher packing density than 11MUA (subsection 4.2) which may have triggered self-quenching of the FITC-GIgG that occupies the binding sites on MIgG antigen and are in close proximity to one another leading to low peak intensity as a case of steric hindrance.
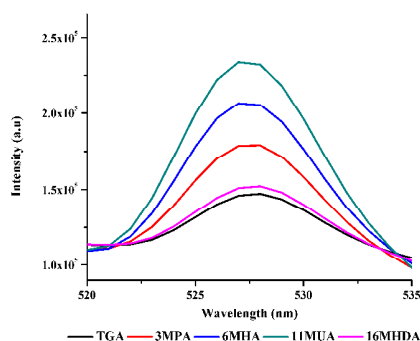
Fig. 9 Fluorescence analysis of FITC-GIgG bound to antigen terminated surfaces of different *n*-alkanethiol.

Conclusions

SAMs of different chain lengths of *n*-alkanethiol were covalently immobilized on 1cm x 1cm gold coated surfaces to form well packed monolayers. FTIR analysis proves greater packing density in higher *n*-alkanethiols. From BCA study, the highest antibody immobilization was observed in *n*=11, 16 alkanethiol where densely packed SAM was formed. Alkanethiol with chain lengths *n*=2, 3 have less antibody immobilized on SAM surface due to loosely packed nature of SAM. Antigen estimation achieved by TMB assay revealed that antigen binding efficiency greatly increased upto *n*=11 SAM. Beyond *n*=11 no increase in antigen binding was observed. Also, fluorescence spectroscopy analysis reveals that the fluorophore intensity of the FITC-secondary antibody increases with increasing *n*-alkanethiol chain length except for 16MHDA. Densely packed antibodies on the surface of 16MHDA SAM had steric problems which restricted its antigen capturing capacity.

It is important to note at this point that the antigen binding efficiency mostly depends on the positioning of the antibody on the solid surface. SE and AFM coupled with TMB assay data show that the orientation of antibody is proper, predominantly the "Flat-On" orientation in case of *n*=2, 3 chain length alkanethiol and favorable "Side-On" orientations were observed with *n*=11 chain length. Finally, this study provides a proof of the fact the increasing chain lengths of the alkanethiols provide increasing antibody binding but upto *n*=11 after which the orientation of the antibody becomes the major factor in antigen binding. Thus, the importance of optimizing the chain lengths of the alkanethiols for antibody-antigen binding is underlined.

Acknowledgements

References

1.   N. Kien Cuong, *Advances in Natural Sciences: Nanoscience and Nanotechnology*, 2012, **3**, 045008.
2.   A. W. Snow, G. G. Jernigan and M. G. Ancona, *Analyst*, 2011, **136**, 4935-4949.
3.   V. Crivianu-Gaita and M. Thompson, *Biosensors and Bioelectronics*, 2015, **70**, 167-180.
4.   X. Zhao, F. Pan, L. Garcia-Gancedo, A. J. Flewitt, G. M. Ashley, J. Luo and J. R. Lu, *Journal of The Royal Society Interface*, 2012, **9**, 2457-2467.
5.   Y. M. Bae, B.-K. Oh, W. Lee, W. H. Lee and J.-W. Choi, *Biosensors and Bioelectronics*, 2005, **21**, 103-110.
6.   Z. Wang and G. Jin, *Journal of Biochemical and Biophysical Methods*, 2003, **57**, 203-211.
7.   F. Hucklebridge, *Journal of Chemical Technology & Biotechnology*, 1996, **66**, 105-105.
8.   X. Zhao, F. Pan, B. Cowsill, J. R. Lu, L. Garcia-Gancedo, A. J. Flewitt, G. M. Ashley and J. Luo, *Langmuir*, 2011, **27**, 7654-7662.
9.   H. Xu, J. R. Lu and D. E. Williams, *The Journal of Physical Chemistry B*, 2006, **110**, 1907-1914.
10.   J. R. Lu, X. Zhao and M. Yaseen, *Current Opinion in Colloid & Interface Science*, 2007, **12**, 9-16.
11.   X. Zhao, F. Pan and J. R. Lu, *Journal of The Royal Society Interface*, 2009, **6**, S659-S670.
12.   B. D. Booth, S. G. Vilt, C. McCabe and G. K. Jennings, *Langmuir*, 2009, **25**, 9995-10001.
13.   B. Wang and H. Haick, *ACS Applied Materials & Interfaces*, 2013, **5**, 5748-5756.
14.   K. Tanaka, K. Ishikawa, K. Nozaki, N. Urakami and T. Yamamoto, *Polym. J*, 2008, **40**, 1017-1024.
15.   N. K. Chaki and K. Vijayamohanan, *Biosensors and Bioelectronics*, 2002, **17**, 1-12.
16.   A. W. Rosenbaum, M. A. Freedman, S. B. Darling, I. Popova and S. J. Sibener, *The Journal of Chemical Physics*, 2004, **120**, 3880-3886.
17.   S. Wu, H. Liu, T. Cheng, X. Zhou, B. Wang, Q. Zhang and X. Wu, *Sensors and Actuators B: Chemical*, 2013, **186**, 353-359.
18.   E. E. Bedford, S. Boujday, V. Humblot, F. X. Gu and C.-M. Pradier, *Colloids and Surfaces B: Biointerfaces*, 2014, **116**, 489-496.
19.   C. D. Bain, J. Evall and G. M. Whitesides, *Journal of the American Chemical Society*, 1989, **111**, 7155-7164.
20.   E. B. Troughton, C. D. Bain, G. M. Whitesides, R. G. Nuzzo, D. L. Allara and M. D. Porter, *Langmuir*, 1988, **4**, 365-385.
21.   C. D. Bain, E. B. Troughton, Y. T. Tao, J. Evall, G. M. Whitesides and R. G. Nuzzo, *Journal of the American Chemical Society*, 1989, **111**, 321-335.
22.   M. D. Porter, T. B. Bright, D. L. Allara and C. E. D. Chidsey, *Journal of the American Chemical Society*, 1987, **109**, 3559-3568.
23.   J. Spinke, M. Liley, F. J. Schmitt, H. J. Guder, L. Angermaier and W. Knoll, *The Journal of Chemical Physics*, 1993, **99**, 7012-7019.
24.   Y. Lee, E. K. Lee, Y. W. Cho, T. Matsui, I.-C. Kang, T.-S. Kim and M. H. Han, *PROTEOMICS*, 2003, **3**, 2289-2304.
25.   M. Mora, J. Wehmeyer, R. Synowicki and C. Garcia, in *Biological Interactions on Materials Surfaces*, eds. D. A. Puleo and R. Bizios, Springer US, 2009, DOI: 10.1007/978-0-387-98161-1_2, ch. 2, pp. 19-41.
26.   H. Fujiwara, in *Spectroscopic Ellipsometry*, John Wiley & Sons, Ltd, 2007, DOI: 10.1002/9780470060193.ch3, pp. 49-79.
27.   Y. Zhuang, Q. Zhu, C. Tu, D. Wang, J. Wu, Y. Xia, G. Tong, L. He, B. Zhu, D. Yan and X. Zhu, *Journal of Materials Chemistry*, 2012, **22**, 23852-23860.
28.   P. K. Smith, R. I. Krohn, G. T. Hermanson, A. K. Mallia, F. H. Gartner, M. D. Provenzano, E. K. Fujimoto, N. M. Goeke, B. J. Olson and D. C. Klenk, *Analytical Biochemistry*, 1985, **150**, 76-85.
29.   C. S. Theegala and A. A. Suleiman, *Microchemical Journal*, 2000, **65**, 105-111.
30.   F. Schreiber, *Progress in Surface Science*, 2000, **65**, 151-257.
31.   S. D. Techane, L. J. Gamble and D. G. Castner, *The Journal of Physical Chemistry C*, 2011, **115**, 9432-9441.
32.   E. Briand, M. Salmain, C. Compère and C.-M. Pradier, *Colloids and Surfaces B: Biointerfaces*, 2006, **53**, 215-224.
33.   C. Chung and M. Lee, *BULLETIN-KOREAN CHEMICAL SOCIETY*, 2004, **25**, 1461-1462.
34.   D. K. Aswal, S. Lenfant, D. Guerin, J. V. Yakhmi and D. Vuillaume, *Analytica Chimica Acta*, 2006, **568**, 84-108.
35.   R. K. Mendes, R. S. Freire, C. P. Fonseca, S. Neves and L. T. Kubota, *Journal of the Brazilian Chemical Society*, 2004, **15**, 849-855.
36.   S. Chah, J. Yi, C. M. Pettit, D. Roy and J. H. Fendler, *Langmuir*, 2001, **18**, 314-318.
37.   C. E. D. Chidsey and D. N. Loiacono, *Langmuir*, 1990, **6**, 682-691.
38.   F. C. Meldrum, J. Flath and W. Knoll, *Langmuir*, 1997, **13**, 2033-2049.
39.   G. T. Hermanson, in *Bioconjugate Techniques (Second Edition)*, ed. G. T. Hermanson, Academic Press, New York, 2008, DOI: http://dx.doi.org/10.1016/B978-0-12-370501-3.00003-5, pp. 213-233.
40.   B. L. Frey and R. M. Corn, *Analytical Chemistry*, 1996, **68**, 3187-3193.
41.   K. Ohtsuka, M. Kuroki, T. Nojima, M. Waki and S. Takenaka, *Analytical Sciences*, 2005, **21**, 215-218.
42.   R. E. Fernandez, E. Bhattacharya and A. Chadha, *Applied Surface Science*, 2008, **254**, 4512-4519.
43.   S. K. Vashist, R. Raiteri, R. Tewari, R. P. Bajpai and L. M. Bharadwaj, *Journal of Physics: Conference Series*, 2006, **34**, 806.
44.   A. Kamyshny, S. Lagerge, S. Partyka, P. Relkin and S. Magdassi, *Langmuir*, 2001, **17**, 8242-8248.
45.   A. Kausaite-Minkstimiene, A. Ramanaviciene, J. Kirlyte and A. Ramanavicius, *Analytical Chemistry*, 2010, **82**, 6401-6408.
46.   D.-S. Wang, C.-C. Chang, S.-C. Shih and C.-W. Lin, *Biomedical Engineering: Applications, Basis and Communications*, 2009, **21**, 303-310.
47.   A. Tronin, T. Dubrovsky and C. Nicolini, *Langmuir*, 1995, **11**, 385-389.
48.   M. Yoon, H. J. Hwang and J. H. Kim, *Journal of Biomedical Science and Engineering*, 2011, **4**, 242.

49.   D. Nečas and P. Klapetek, *centr.eur.j.phys.*, 2012, **10**, 181-188.
50.   H. Kim, D.-Y. Kang, H.-J. Goh, B.-K. Oh, R. P. Singh, S.-M. Oh and J.-W. Choi, *Ultramicroscopy*, 2008, **108**, 1152-1156.
51.   R. J. Green, J. Davies, M. C. Davies, C. J. Roberts and S. J. B. Tendler, *Biomaterials*, 1997, **18**, 405-413.
52.   W. Schramm, S.-H. Paek and G. Voss, *ImmunoMethods*, 1993, **3**, 93-103.
53.   H. Oneda and K. Inouye, *Bioscience, Biotechnology, and Biochemistry*, 2004, **68**, 2190-2192.
54.   C. Deka, B. E. Lehnert, N. M. Lehnert, G. M. Jones, L. A. Sklar and J. A. Steinkamp, *Cytometry*, 1996, **25**, 271-279.

Graphical Abstract:
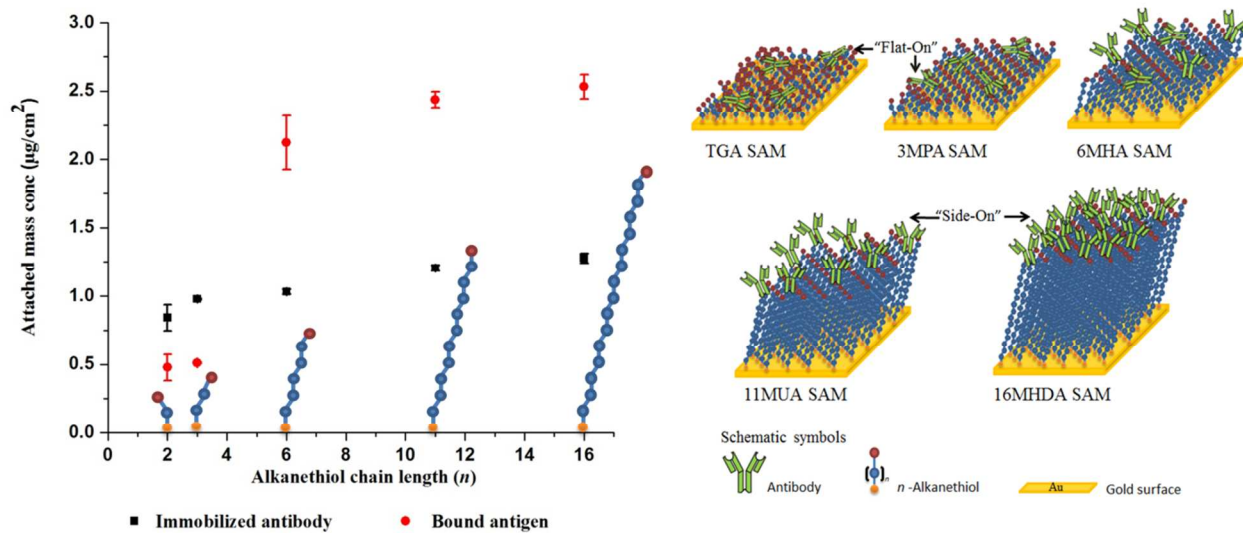
- Antibody immobilization efficiency varied with SAM of *n*-alkanethiols. However, this did not necessarily result in corresponding increase in antigen binding.